Resonant x-ray magnetic scattering from $U_{1-x}Np_xRu_2Si_2$ alloys

E. Lidström and D. Mannix
European Synchrotron Radiation Facility, Boîte Postale 220, F-38043 Grenoble Cedex, France
and European Commission, JRC, Institute for Transuranium Elements, Postfach 2340, D-76125 Karlsruhe, Germany

A. Hiess
Institut Laue Langevin, Boîte Postale 156, F-38042 Grenoble Cedex, France

J. Rebizant, F. Wastin, and G. H. Lander
European Commission, JRC, Institute for Transuranium Elements, Postfach 2340, D-76125 Karlsruhe, Germany

I. Marri
European Synchrotron Radiation Facility, Boîte Postale 220, F-38043 Grenoble Cedex, France
and INFM and Dipartimento di Fisica dell'Università, Modena, 41100 Modena, Italy

P. Carra and C. Vettier
European Synchrotron Radiation Facility, Boîte Postale 220, F-38043 Grenoble Cedex, France

M. J. Longfield
Department of Physics, Oliver Lodge Laboratory, University of Liverpool, Oxford Street, Liverpool L69 7ZE, United Kingdom
(Received 21 May 1999)

We have studied $U_{1-x}Np_xRu_2Si_2$ alloys with $x=0.1$, 0.5, and 1.0 using resonant x-ray magnetic scattering. For the $x=1$ neptunium compound we have confirmed previous neutron scattering results, but with much higher count rates and improved q resolution. Using the element specificity of the method, we have found that the temperature dependence of the uranium and the neptunium moments differ in the mixed $U_{1-x}Np_xRu_2Si_2$ solid solutions and we present some tentative explanations for this behavior. In principle, by measuring the responses at the individual M edges we are able to determine the ratio of the magnetic moments on the two magnetic species in the random alloys. The observed variation of intensity versus energy is compared to a calculation of a $x=0.50$ alloy using a localized model and a coherent superposition of U^{4+} and Np^{3+} ions. The agreement between theory and experiment is reasonable, suggesting a ratio $\mu_U/\mu_{Np}\sim 0.25$ in this alloy. Since μ_{Np} is known to be $1.5\mu_B$ for $0.10\leqslant x\leqslant 1$, the uranium moment is $\sim 0.4\mu_B$. This is much larger than $0.02\mu_B$ known to exist in URu_2Si_2 $(x=0)$. The increase is a consequence of the molecular field of the ordered Np^{3+} moments and is consistent with the crystal-field model proposed for the U^{4+} ground state.

I. INTRODUCTION

The $U_{1-x}Np_xRu_2Si_2$ solid solutions for all x crystallize in the tetragonal $ThCr_2Si_2$ structure, with space group $I4/mmm$. The $x=0$ compound URu_2Si_2 ($a=4.131$ Å, $c=9.574$ Å) is a well known heavy fermion superconductor with $T_N=17.5$ K and $T_c=1.2$ K.[1,2] It orders in a simple antiferromagnet structure with propagation vector $\mathbf{q}=(0\,0\,1)$ and the direction of the moments along the c axis. The crystal and magnetic structures are displayed in Fig. 1. The ordered moment of URu_2Si_2 is only about $0.02\mu_B$ (Ref. 2) compared to a normal uranium moment in an alloy of at least $1\mu_B$. There is a considerable jump in specific heat at T_N and a major difficulty is how to reconcile this jump with such a small moment. It has therefore been argued that the true order parameter is not the magnetic moment but one of quadrupole nature.[3–5] The electronic specific heat has been estimated to be between 23 and 180 mJ/(mol K^2) (Ref. 2). The valence state of uranium is still an open question. Broholm *et al.*[6] interpreted their inelastic neutron scattering data by assuming that the two lowest lying states are nonmagnetic singlets. The valence state must then be $4^+(5f^2)$. In contrast, a 3^+ valence state $(5f^3)$ has an uneven number of electrons and all levels are at least twofold degenerate. A nonmagnetic singlet ground state can also be the basis for explaining the low value of the ordered magnetic moment. A small moment is achieved by applying an internal or external field on the singlet ground state and inducing a moment by mixing the wave functions with those of higher (magnetic) states.[7] Fåk *et al.*,[2] however, state that the data of Broholm *et al.*[6] could equally well be explained with a scheme where the two lowest states are doublets. Santini and Amoretti[3,8] have used a model with a U^{4+} valence state to explain magnetization data obtained by Sugiyama *et al.*[9] amongst others. A number of metamagnetic transitions are observed[9] above about 36 T ending with a ferromagnetic state above 39.6 T. The uranium moment approaches $2\mu_B$ as the field is raised close to 60 T. However, a major difficulty with assuming a $5f^2$ configuration is that band structure calculations of the electronic state based on the local spin density approximation generally give slightly less than 3 $5f$ electrons associated with the uranium atom in such intermetallic

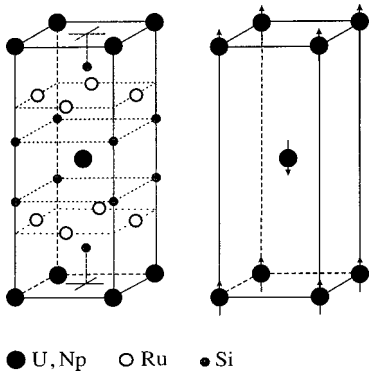

FIG. 1. The $ThCr_2Si_2$ crystal structure. The arrows show the magnetic structure corresponding to a wave vector $q=[0\,0\,1]$, which is found for $0 \leqslant x \leqslant 0.90$. For URu_2Si_2 the lattice parameters are $a=4.131$ Å, $c=9.574$ Å.

compounds[10,11] indicating that a 3^+ valence state may be a closer description of the uranium electronic configuration.

The $x=1$ compound $NpRu_2Si_2$ ($a=4.137$ Å, $c=9.593$ Å), orders antiferromagnetically at $T_N=27.5$ K and has been studied with neutron scattering and Mössbauer spectroscopy.[12] The structure is incommensurate with a propagation vector $\mathbf{q}=(00k)$ and the moments along the c axis; k increases from 0.760(5) close to T_N, to 0.865(5) at $T=1.3$ K. A third-order harmonic magnetic satellite was observed with neutron scattering at 1.3 K showing that the structure squares up with decreasing temperature. The amplitude of the first harmonic was found to be $1.7(2)\mu_B$.

To obtain additional information on the ground state of URu_2Si_2, perturbing the system through alloying is a potentially fruitful approach. A number of studies have been performed with substitutions of the uranium or the ruthenium (for references, see Ref. 13). Of the possible substitutions on the uranium site, that with neptunium (the next element after uranium) is the most gentle due to the closeness of the atomic size and chemical properties. The $U_{1-x}Np_xRu_2Si_2$ series with $0.1<x<1.0$ has been studied with Mössbauer spectroscopy by Zwirner *et al.*[14] and the transport properties have been examined by Wastin *et al.*[13] Some of these data are summarized in Fig. 2. As shown in Fig. 2(a), the neptunium magnetic moment stays almost constant around $1.5\mu_B$ for all $x \geqslant 0.1$. This is somewhat surprising, given the difference in the moments of the two parent compounds. The moment is always aligned along the c axis. The Néel temperature, Fig. 2(b), varies smoothly with the neptunium content and the isomer shift stays constant over the series, Fig. 2(c). By comparing the isomer shift to that of the reference compound $NpAl_2$, taking into account the fact that the alloys are metallic,[15] it is found that the neptunium is in the Np^{3+} valence state in the whole series. Finally, the unit cell volume, Fig. 2(d), is almost constant as a function of x. Neutron scattering has been used to examine the $x=0.9$ sample.[16] At this doping the order changes from incommensurate to commensurate and the total moment is consistent with $\mu_U \leqslant 0.5\mu_B$. The neutron intensities are, of course, proportional to the *average* moment in the material and are not element specific.

Nonresonant magnetic x-ray scattering is many orders of magnitude weaker than x-ray charge scattering. When the

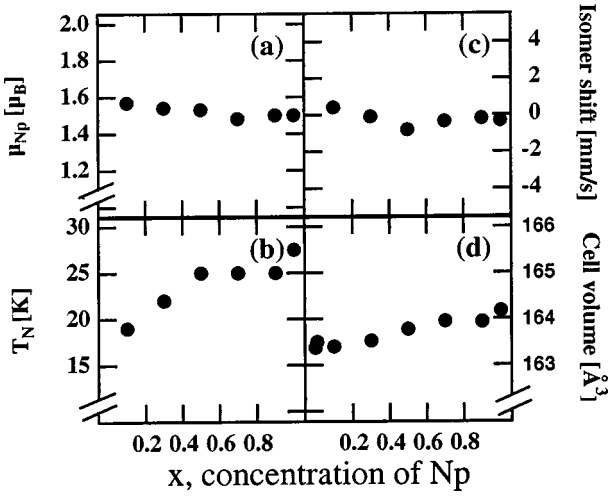

FIG. 2. The neptunium ordered moment (a), the transition temperature (b), the isomer shift (c), and the unit cell volume (d), for the $U_{1-x}Np_xRu_2Si_2$ series. From Zwirner *et al.* (Ref. 14) (a)–(c) and Wastin *et al.* (Ref. 13) (d).

x-ray energy is tuned to an absorption edge, strong enhancements of the magnetic intensity have been observed, especially at the rare earth L edges (50 times) and the actinide M edges. In the latter, an enhancement of $\sim 10^7$ has been seen in UAs.[17] Because of the resonant process,[18] the method is element specific so that the contribution to the magnetism of each species can be probed separately.

In comparison with neutrons, limitations of resonant x-ray magnetic scattering (RXMS) are (a) that the enhancement at the resonance is unknown, so that it is not possible to determine the size of the ordered moment, and (b) that because the energy is at a resonance there is large absorption. The latter necessitates complex corrections and means that the technique is near surface sensitive with penetration depths (for actinides at the M edges) of ~ 1000 Å.

To address the relationship between the resonant enhancement and the magnetic moments we have performed theoretical calculations, also presented in this paper. It is important to bear in mind two aspects of this problem. The first is that we are addressing transitions that are essentially dipole in nature, from the $3d$ core state to the partially filled $5f$ state. Complications of quadrupole transitions are therefore avoided; in addition, the principal magnetic signal arises from the unfilled $5f$ shell in these actinide materials. The second simplification is that we are not attempting to place the calculations on an absolute scale; rather we are interested in the ratio of the enhancement at the neptunium site in comparison to that at the uranium site. We may then use the fact that the Mössbauer hyperfine field gives the neptunium moment to obtain approximate values for the uranium moment and thus compare them to the small value found in the pure ($x=0$) compound URu_2Si_2.

II. EXPERIMENTAL TECHNIQUE

The work reported here was performed on the ID20 magnetic scattering beamline at the ESRF. The x-ray beam is provided by undulators that give a narrow beam with small divergence. It is then further concentrated by two silicon

mirrors providing vertical focusing, and a second crystal in the monochromator assembly, which can be curved to provide sagittal focusing. The mirrors cut off higher order wavelength harmonics from the undulator source. The monochromator crystals are made of silicon with reflecting (1 1 1) planes and the energy width of the beam in the range used in this study was 0.52(2) eV. A monochromatic beam with a flux of $\sim 5\times 10^{11}$ photons/s at 3.7 keV can be concentrated on a 0.3×0.2 mm^2 (horizontal$\times$vertical) spot at the sample position. The linear polarization of the beam is $99\pm 1\%$.

The $U_{1-x}Np_xRu_2Si_2$ single crystals were selected from as-quenched bulk samples obtained as described in Ref. 13. The crystals were oriented and mounted on 2×2 mm^2 germanium (1 1 1) wafer, and sealed under beryllium caps at the ITU in Karlsruhe. They were loaded in a helium closed cycle refrigerator (CCR) at the ESRF. The diffractometer was used in the vertical geometry with incoming σ polarization. Because of safety concerns, the samples cannot be aligned optically. After mounting the sample assembly in the CCR on the diffractometer, a charge peak from the underlying germanium wafer was found. The intensity of this charge peak from the wafer was then monitored as a function of the (x,y) position on the germanium wafer. When the photon beam is incident on the samples there is a sharp drop in the intensity because of the absorption, and this allows the position of the small actinide samples (between 0.3 and 0.6 mm on edge, but irregular in shape) to be determined. The crystals used, $NpRu_2Si_2$, $U_{0.5}Np_{0.5}Ru_2Si_2$, and $U_{0.9}Np_{0.1}Ru_2Si_2$ each had a volume of about 0.1 mm^3. The $x=1.0$ and 0.5 samples turned out to be of excellent quality, whereas the $x=0.1$ sample consisted of a large number of grains which somewhat hampered the experiment. Previous measurements on these materials[13] using x-ray diffraction, metallography, and microprobe analysis have shown them to be homogeneous.

The raw data have been corrected for the absorption caused by the beryllium (2×0.40 mm plus the oblique beam path through a flat 0.2 mm sample cap), air and Kapton ($50\mu m$) in the beamline as well as for the Lorentz factor. These corrections are accurate and vary by a factor of ~ 4 on changing the energy from 3.5 to 4.0 keV.

III. MAGNETIC STRUCTURES

A. $NpRu_2Si_2$ ($x=1$)

The energy was tuned to the neptunium M_4 edge at 3.844 keV and scans were performed along the c^* direction. Our results for $NpRu_2Si_2$ agree with those obtained by Bogé *et al.*[12] using neutron scattering. The compound orders in a longitudinal incommensurate structure with the moments modulated along the c axis. The value of the incommensurate propagation vector is displayed in Fig. 3(a). It is close to the commensurate value of 0.75 at the Néel temperature and increases linearly below T_N as a function of temperature with no indication of saturation. The linear behavior was found to continue to 1.3 K in the neutron study. Over the range in which the two technique have been used the results are in good agreement, see Fig. 3(a).

As the temperature is lowered, the observation of third-order magnetic satellites, Fig. 3(b), shows that the magnetic structure approaches a square wave. The first-order harmonic grows with $\beta=0.31(5)$ as the temperature is lowered. This

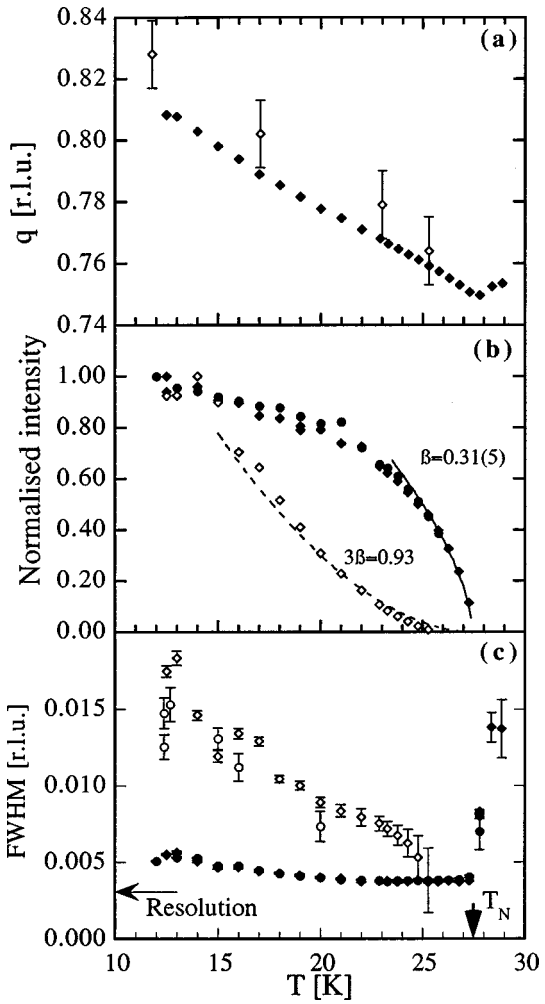

FIG. 3. Details of the magnetic structure for the $x=1$ sample as a function of temperature. (a) shows the magnetic propagation vector. The open symbols are the data of Bogé *et al.* (Ref. 12). The errors for our data are smaller than the symbols. (b) shows the normalized intensities of the first- and third-order satellites at the M_4 and M_5 edges. The solid line is a fit to the first-order satellites in the interval $25.3<T<27.3$ K. The broken line is the third power of this function times a scale factor. Filled diamonds: first-order satellites at the M_4 edge, filled circles: first-order satellites at the M_5 edge, open diamonds: third-order satellites at the M_4 edge. (c) FWHM (1 r.l.u.$=0.656$ Å^{-1} along the c axis) of the first- and third-order satellites at $(0\ 0\ 4+q)$ for the two edges. Diamonds M_4 edge, circles M_5 edge; Filled symbols first-order satellites, open symbols third-order satellites.

is close to the values found for USb and UTe and agrees with the value of $5/16=0.3125$ of a three-dimensional Ising system.[19] The third-order satellite grows approximately as the third power of the first-order satellite, as predicted by mean-field theory[20] (for such a model β should be 0.5). The width of the magnetic first-order peak increases slightly as the temperature is lowered whereas it grows substantially for the third-order satellite [Fig. 3(c)]. Our interpretation is that the competition between the strain and the magnetic terms in the energy leads to a compromise such that regions over which a perfect (incommensurate) magnetic modulation exist become shorter as the moment increases at lower temperatures. This leads to a broadening of the Bragg peak as a function of temperature, as observed also in the work by

Helgesen *et al.* on holmium.[21] From the half width at half maximum (HWHM) of the first harmonic, we estimate a correlation length along the c axis of $\xi_c \approx 650$ Å at $T=12.5$ K.

We notice that FWHM$(3\mathbf{q}) \approx 3 \times$ FWHM$(\mathbf{q})$ at low temperature. According to Axe,[22] the widths of higher-order satellites should be proportional to n^2 where n is the order of the harmonic. This is not the case here where an approximate linear behavior is observed, but is obvious that fifth-order satellites would be even broader than the third-order ones. We obtain an integrated intensity ratio between the third-order and first-order satellites at (0 0 4.424) and (0 0 4.808), respectively, of 1.5% at 12.5 K (5800 and 1.1×10^6 cts/s at the peaks). Assuming that the integrated intensity of the third-order satellite grows with $[(T_N-T)/T_N)]^{(2\times3\beta)}$, and that the structure would be a perfect square wave at 0 K, a calculation gives the value of 2.2% at 12.5 K. We estimate a fifth-order satellite peak intensity of 1000–3000 cts/s in the same way. Unfortunately, in our experiment, for the accessible temperature range, the fifth-order satellites fall close to the (0 0 4) charge reflection and none were detected. If the temperature could be lowered further in a future experiment, the satellite would move further away from the charge peak, as well as becoming stronger, and it might be possible to observe it.

We also searched for second-order charge satellites, which would correspond to a magnetoelastic distortion but no such reflection could be observed. Of course, magnetoelastic strain in a tetragonal system may also be accommodated by a change in the c/a ratio below T_N, but an examination of this quantity is difficult in these experiments as the specular face of the crystal is (0 0 l).

B. The mixed compounds

Using neutron scattering it has been shown[16] that at $x=0.9$, the alloy orders (at low temperature) in the same commensurate antiferromagnetic structure as the $x=0$ compound, see Fig. 1. Only a small amount of uranium is thus enough to turn the magnetic structure commensurate and the $x=0.1$ and $x=0.5$ compounds in this study are both commensurate, as previously suggested by Mössbauer spectroscopy.[14] Because of the element sensitivity of the RXMS method we can investigate the magnetism of the two species separately. The (0 0 3) and (0 0 5) magnetic reflections were studied as a function of temperature with the energy tuned to the respective M_4 edges of the two elements. For the $x=0.5$ compound, we performed L scans and θ rocks (i.e., scans along the L direction in reciprocal space and scans of the θ angle) to obtain the integrated intensity.

In principle it should be possible to deduce the c axis magnetic correlation length ξ_c from the widths of scans along the L direction. The linewidths in the L scans (FWHM) were found to be 0.0037(1) and 0.0022(1) reciprocal lattice units (r.l.u.) for the uranium M_4 edge at the (0 0 3) and (0 0 5) reflections, respectively, and they were constant as a function of temperature. For the neptunium M_4 edge we find a width of 0.0035(1) r.l.u. at the (0 0 3) reflection. If, however, we multiply the FWHM with $\sin\theta_B$ where θ_B is the Bragg angle, we find a constant value for the uranium data (only one reflection was measured at the neptunium edge). At the actinide M edges the absorption is very large and the absorption length ($1/\mu \sim 0.5$ μm, see below) is shorter than the probe coherence length [defined as $\lambda/(\Delta\lambda/\lambda)$ and in our case $\sim 2\mu$m]. In this situation the profiles of the peaks tend to be related to the Bragg angle (as we find) but the HWHM values cannot be easily related to the correlation length, as discussed recently by Bernhoeft.[23] In the case of a ''perfect'' crystal (i.e., one with a very small mosaic) the HWHM can be related to $(1/\mu)$ but as the crystal mosaic increases even this becomes more complicated. In the case of the $x=1$ sample, which is incommensurate, the correlation length of ~ 650 Å is the defining length scale, whereas the much longer magnetic correlation lengths in the (commensurate) $x=0.5$ and $x=0.1$ samples takes one into the limit in which the absorption length becomes the shortest length scale. To determine the correlation length ξ in well ordered actinide compounds it is necessary to go off resonance, which lowers the absorption as well as the intensity.

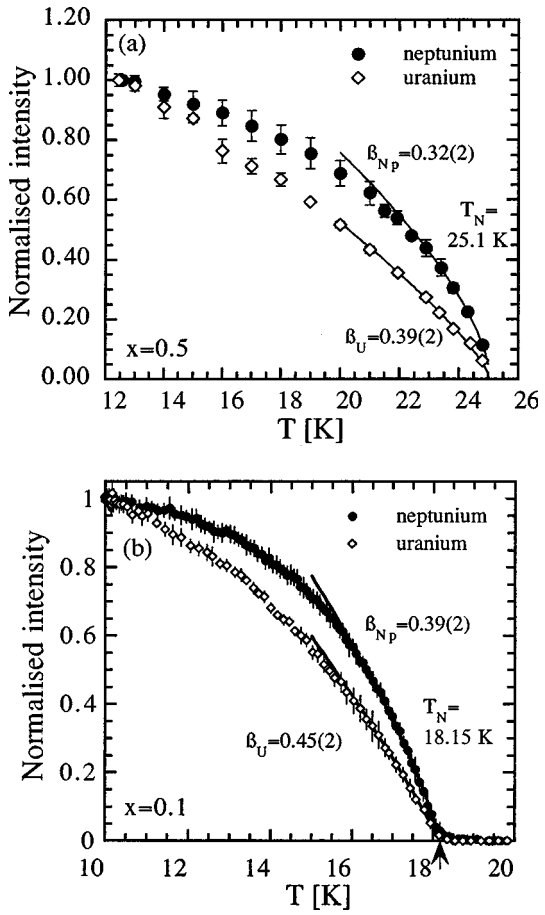

FIG. 4. The integrated intensity for the two atomic species in the mixed samples. The data have been normalized at the lowest temperature. (a) $x=0.5$; the points are the average of L and θ scans at the (0 0 3) and (0 0 5) reflections. The solid lines are fits to the data in the 23–25 K region. (b) $x=0.1$; the results of a large number of temperature scans at the (0 0 5) peak. The solid lines are fits to the data above 17 K.

The temperature dependencies are displayed in Fig. 4 and are normalized to 1 at $T=12.5$ K and 10 K for the $x=0.5$ and 0.1 samples, respectively. The observation of a difference in the temperature behavior was verified in our subsequent study of the $x=0.1$ sample. For this compound, we

measured the peak intensity of a large number of grains as a function of the temperature and normalized the intensity at 10 K, see Fig. 4(b). This was done at the uranium and neptunium M_4 edges as well as at the neptunium M_5 edge. It is worth emphasizing that in no scan did the uranium data overlap with the neptunium ones in the intermediate temperature region.

Fits to the data close to T_N give the critical exponents $\beta_{Np}=0.32(2)$ and $\beta_U=0.39(2)$ in the $x=0.5$ sample. For the $x=0.1$ sample the values are 0.39(2) and 0.45(2). For a particular composition, the Néel temperature was found to be identical for the two species within the experimental resolution (<0.1 K).

IV. ENERGY DEPENDENCE

A. The resonant process

The intense magnetic scattering at the actinide M_4 and M_5 energies is due to the resonant enhancement at the absorption edges as described by Hannon *et al.*[18] In the dipole approximation, the resonances couple the $3d_{3/2}$ and $3d_{5/2}$ levels (M_4 and M_5 edges) to the $5f$ electrons. The strength of a resonance depends on the probability of the initial state, the probability that the excited level is vacant and on the partial width for electric dipole radiative decay from the excited state to the initial state. The resonant amplitude has the form

$$f \propto \frac{a_1}{(E_r-\hbar\omega)/(\Gamma_r/2)-i} - \frac{a_2}{(E_r+\hbar\omega)/(\Gamma_r/2)+i} \qquad (1)$$

for each resonance at E_r with a lifetime defined by Γ_r. The second term can be neglected in the further developments it does not contribute to the resonant behavior. In our particular case, we get

$$\begin{aligned} I(\hbar\omega) = \sin^2\theta \Bigg\{ & \left[\frac{E_4}{\hbar\omega} \frac{A_4}{1+[(E_4-\hbar\omega)/(\Gamma_4/2)]^2} + \frac{E_5}{\hbar\omega} \frac{A_5}{1+[(E_5-\hbar\omega)/(\Gamma_5/2)]^2} \right]^2 \\ & + \left[\frac{E_4}{\hbar\omega} \frac{A_4}{1+[(E_4-\hbar\omega)/(\Gamma_4/2)]^2} \left[\frac{E_4-\hbar\omega}{\Gamma_4/2} \right] \right. \\ & \left. + \frac{E_5}{\hbar\omega} \frac{A_5}{1+[(E_5-\hbar\omega)/(\Gamma_5/2)]^2} \left[\frac{E_5-\hbar\omega}{\Gamma_5/2} \right] \right]^2 \Bigg\} \end{aligned} \qquad (2)$$

for two resonances, M_4 and M_5, for the pure neptunium compound (see Blume[24]). This expression is valid for dipole resonances with the propagation vector parallel to the moment direction which is the case in our experiments. The $\sin^2\theta$ factor comes from the angle between the moment direction and the outgoing wave vector. A_4, E_4, and Γ_4 are the amplitude, the resonant energy and the full width of the M_4 resonance, similarly for the M_5 resonance.

In the mixed compounds with two actinide elements present there are four interfering resonances and in the general case, we fit to the expression

$$\begin{aligned} I = |f|^2 &= \sin^2\theta \left(\sum_r F_r^1 \right)^* \left(\sum_r F_r^1 \right) \\ &= \sin^2\theta \left(\sum_r \frac{E_r}{\hbar\omega} \frac{A_r}{(E_r-\hbar\omega)/(\Gamma_4/2)+i} \right) (\text{c.c.}), \end{aligned} \qquad (3)$$

where the F_r^1 describe each dipole resonance. In the case of actinide M edges all resonant scattering investigated has been found to be due to dipole resonances. The thermal evolution of the dipole magnetic scattering is proportional to the square of the magnetic order parameter,[25] but the resonant enhancement (i.e., the proportionality factor) is unknown. This implies that we can only put our magnetic intensity on a relative scale and not extract the value of the moment. However, we can measure element specific effects, such as the temperature dependence, related to the $5f$ moments. Similar experiments have been reported in the lanthanides,[26] but are done at the L edges, where the dominant dipole resonances are connected to the $5d$ states rather than to the primary magnetism of the $4f$ shell.

Data were obtained using fixed-q scans for all three samples, i.e., observing the peak intensity of a magnetic reflection as a function of the x-ray energy. A better, but more time consuming, way is to measure the integrated intensity at each energy using Q scans. Both methods were used for the $x=0.1$ sample and were found to give similar results.

B. Absorption

As stated earlier, the data have been corrected for absorption by the Kapton, air, and beryllium, all of which have a gradual dependence on the energy and are well known. Much more difficult is to correct for self-absorption by the sample. This is a sharply peaked function corresponding to the white lines at the M_4 and M_5 edges. Recent work on thin films of UO_2 (Ref. 27) shows that previous estimates, mainly from fluorescence measurements, of the intensity of these white lines obtained values too low by a factor of ~ 2. For the actinides, and especially for transuranium samples, these measurements are difficult; suitable samples, i.e., thin films, do not exist and the energies $3<\hbar\omega<4$ keV are not in the standard range used for absorption spectroscopy. A rough measure of the fluorescence may be obtained by plotting the background in each scan as a function of energy. These data show that the position of the white lines and the maximum of the resonant enhancement coincide for our samples. This has been the case for actinide samples studied previously.

To extract $\mu(\hbar\omega)$ we chose to use the UO_2 data[23,27] for both elements as these are the most reliable available. We thus assume that the energy dependence of the absorption of neptunium is identical to that of uranium but the energy is shifted. To obtain the neptunium absorption, the UO_2 curves are simply shifted to the M-resonant energies of neptunium. This should be regarded as a first approximation. It should be emphasised that it is only the strong white lines at the resonant energies that are in doubt. The absorption between these ''peaks'' is known from tables. The values include contributions from ruthenium and silicon, neither of which have resonances in this energy range. Figure 5 shows $\mu(\hbar\omega)$ for the $x=0.5$ sample. The FWHM of the white lines are 4.4 eV. In

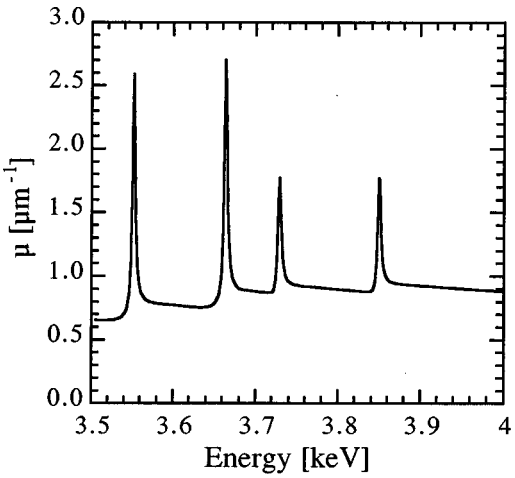

FIG. 5. The absorption μ as a function of energy used to correct the $x=0.5$ data.

the pure neptunium compound the absorption reaches about $4.5\mu\mathrm{m}^{-1}$ at the M_5 edge and $2.65\mu\mathrm{m}^{-1}$ at the M_4. Away from the resonances, the absorption varies between 0.6 and $0.95\mu\mathrm{m}^{-1}$. For the mixed samples the absorption at the edges is reduced in proportion to the concentration.

For the simple case where the sample correlation length is shorter than the absorption length ($\xi \ll 1/\mu$), and also shorter than the probe coherence length, we should multiply our experimental data with μ. As discussed by Bernhoeft,[23] in the case when the absorption length is much *shorter* than the sample correlation length, the data should be corrected with μ^2. From the measurements of the correlation lengths described in the previous section, we know that in the case of the (incommensurate) $x=1.0$ compound, the shortest distance is the correlation length ($\xi \sim 650$ Å $=0.065$ μm) and we should therefore correct with μ. In the $x=0.5$ compound, on the other hand, it is clear that we should use μ^2 *at the resonant energies*. For the $x=0.1$ compound the crystal mosaic was too poor to allow reliable data to be taken. Given that this compound also orders commensurately, and therefore that the correlation length is likely to be large, we find a correction by μ^2 most probable, at least at the uranium M_4 edge where the absorption is large. One weakness of our experiment is that L scans were not systematically performed as a function of energy. It is possible that the data should be corrected by μ^2 at the peaks but that complete and rather complex corrections[23] should be applied off resonance. As we shall see, the differences in the fitted branching ratios are significant, but not dramatic, when we change from μ to μ^2 for the correction.

C. Branching ratios and magnetic moments

We have performed energy scans for all samples. The raw data and the data corrected for μ and μ^2 were fitted to Eq. (3). The interest of the energy scans is twofold. First, the relative intensity of the M_4 and M_5 edges, the branching ratio ($\mathrm{BR}=A_4\Gamma_4/A_5\Gamma_5$), contains information about the electronic ground state of the actinide ions. The ratio depends on the valence state of the ion as well as on the crystal-field parameters. The second information we hope to obtain from the energy scans is the size of the ordered uranium moment. From the Mössbauer study we know that the neptunium moment is almost constant at $1.5\mu_B$ for $x \geqslant 0.10$.

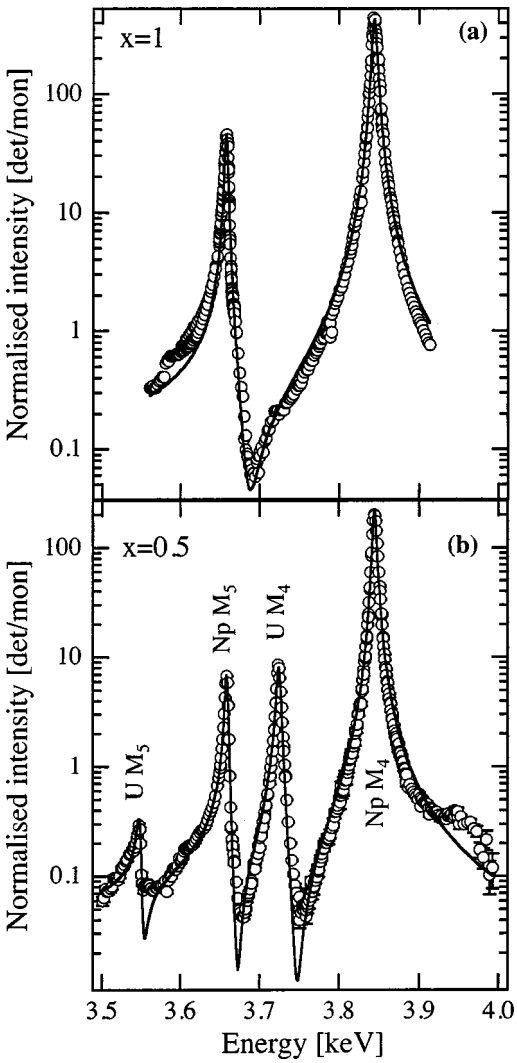

FIG. 6. (a) Results of the $x=1$ fixed-q energy scan of the (0 0 4.808) reflection. The data displayed have been corrected for absorption from beryllium, Kapton and air as discussed in the text, but not for the self-absorption of the sample. The solid line is a fit. Note the logarithmic scale. (b) The fixed-q energy scan data for $x=0.5$. The solid line is a fit.

The data for the $x=1.0$ and $x=0.5$ samples are displayed in Fig. 6. The results of the fits for all three compounds in this study are presented in Tables I and II. In Table II we have marked in bold the branching ratios obtained using what we believe to be the correct self-absorption correction as discussed in the previous section (μ^2 for the $x=0.1$ and $x=0.5$ samples, and μ for the $x=1$ sample). There is a slight shift in the energy for the $x=0.1$ sample, for which the data were obtained at a different occasion from the two other compounds, and therefore with a different energy calibration of the instrument.

The energies are in good agreement with our recent tabulation for the actinides.[28] The peak widths (FWHM) are somewhat narrower than reported earlier[29] for uranium compounds, and part of this can be ascribed to the better energy resolution at ID20 compared to that of the X22C beamline at the NSLS, Brookhaven National laboratory, where we have

TABLE I. Results of the fits to the energy scans of the data before correcting for the self-absorption of the sample, but with all other corrections applied. The absolute energy errors are ±1 eV.

Compound	Resonance	Energy [eV]	Amplitude [arb. units]	FWHM [eV]
$x=0.1$	Np M_4	3846	14.17(4)	5.32(3)
	Np M_5	3661	5.04(7)	3.77(12)
	U M_4	3726	31.82(7)	6.38(2)
$x=0.5$	Np M_4	3844	29.54(6)	5.59(2)
	Np M_5	3659	4.82(5)	4.60(13)
	U M_4	3725	5.41(5)	6.36(12)
	U M_5	3549	0.80(7)	6(1)
$x=1.0$	Np M_4	3844	41.0(4)	7.1(2)
	Np M_5	3659	12.6(3)	4.8(3)

measured previously. The narrowness of the resonance is also intimately connected with the absorption and coherence effects in the incident radiation,[23] so that values of between 5 and as high as 10 eV have been found for uranium resonances. Our values lie within this range, except for those of the neptunium M_5 resonance. However, the widths from the fits at these latter edges have to be taken with some caution. As can be seen from Fig. 6, strong interference effects are observed near the M_5 resonances, thus their exact fitting tends to depend on how well the interference effects are reproduced. This gives us less confidence in the widths of both the uranium and neptunium M_5 resonances.

The branching ratios show, as expected, that the M_4 edge is always the strongest transition. This is because it involves the $5f_{5/2}$ state which will be the one primarily filled for the light actinides. As shown by Tang *et al.*,[29] the largest BR should be with the smallest number of $5f$ electrons, thus the BR for U^{4+} (f^2) should be higher than that for Np^{3+} (f^4). Perhaps surprisingly, the BR values in Table II show little sign of this variation. Although, they rise for the neptunium site going from $x=1.0$ to $x=0.5$, they then decrease at the lowest concentration of $x=0.1$. More systematics of such effects are needed before we can be sure whether this represents a real change in the electronic structure, or whether artifacts in the fitting procedures are causing these differences. We remark that the values of the BR between the 3 and 6 are close to those found previously for USb and, UO_2 by Tang *et al.*,[29] and in that paper is a discussion of how these values indicate the importance of crystal fields. For the free atoms the values for uranium are above 10.

To extract the ratio of the magnetic moments at the uranium and neptunium sites, we compare the relative amplitudes of the signals, and then normalize by the concentration. In both cases this is 0.20(5). As presented below, we have calculated the relative amplitudes of these signals for the $x=0.5$ sample, assuming certain ground states for the uranium and neptunium ions. It is clear, however, that whatever ground state is assumed, the moment on the uranium sites in these systems is considerable. In comparison to the moment of $1.5\mu_B$ known to exist at the neptunium site, a simple linear proportionality would suggest a moment of $\sim 0.2 \times 1.5 = 0.3\mu_B$ at each uranium site, and this is an order of magnitude larger than the $0.02\mu_B$ found in the $x=0$ material.

TABLE II. Branching ratios from fits to intensity data (I) and those corrected for the self-absorption. The values in bold are the preferred ones as discussed in the text. The errors are those of the fitting process and do not take systematic errors into account.

Compound	element	BR (I)	BR ($I\times\mu$)	BR. ($I\times\mu^2$)
$x=0.1$	Np	4.0(2)	3.4(2)	**2.6(1)**
$x=0.5$	Np	7.4(3)	6.9(2)	**6.0(2)**
	U	7(2)	6(1)	**6(2)**
$x=1.0$	Np	4.7(1)	**4.0(1)**	3.1(1)

V. DISCUSSION

A. Crystal-field calculation

This subsection reports numerical crystal-field calculations for resonant magnetic diffraction at the $M_{4,5}$ edges for the $x=0.5$ alloy. Our theoretical spectra were obtained from a simple localized model, consisting of a coherent superposition of two ions: U^{4+} and Np^{3+}. For these, all electric-dipole transitions from the lowest state of the $5f^n$ configuration to the full multiplet $3d^9 5f^{n+1}$ were calculated in the presence of a D_{4h} crystalline environment. Before going into the details of the calculation, basic expressions for the resonant scattering amplitude and cross section will be reviewed for the convenience of the reader.

For any electric 2^L-pole transition in a spherically symmetric ion, the resonant elastic x-ray scattering amplitude can be given the form[25]

$$f^{EL}(\omega) = 4\pi i \sum_{zm} T_m^{(z)*}(\boldsymbol{\epsilon},\mathbf{k},\boldsymbol{\epsilon}'^*,\mathbf{k}')_{EL} \langle g|F_m^{(z)}(\omega)_{EL}|g\rangle, \tag{4}$$

where

$$F_m^{(z)}(\omega)_{EL} = \sqrt{\frac{2z+1}{2L+1}} \sum_{M,M'} C^{LM}_{LM';zm} F^{(e)}_{LM';LM}(\omega), \tag{5}$$

and

$$T_m^{(z)*}(\boldsymbol{\epsilon},\mathbf{k},\boldsymbol{\epsilon}'^*,\mathbf{k}')_{EL} = \sqrt{\frac{2z+1}{2L+1}} \sum_{M,M'} C^{LM}_{LM';zm} [\boldsymbol{\epsilon}'^* \cdot \mathbf{Y}^{(e)}_{LM'}(\mathbf{k}')] \times [\mathbf{Y}^{(e)*}_{LM}(\mathbf{k}) \cdot \boldsymbol{\epsilon}], \tag{6}$$

with

$$F^{(e)}_{LM';LM}(\omega) = \sum_n \frac{1}{2\lambda_{ng}} \left[\frac{J^{(e)\dagger}_{LM'}|n\rangle\langle n|J^{(e)}_{LM}}{E_n - E_g - \hbar\omega - i(\Gamma/2)} \right]_m^z. \tag{7}$$

The notation is as follows: $\boldsymbol{\epsilon},\mathbf{k}$ and $\boldsymbol{\epsilon}',\mathbf{k}'$ denote incident and final photon polarizations and wave vectors, respectively; $C^{LM}_{LM';zm}$ represents a Clebsch-Gordan coefficient. The current operator $J^{(e)}_{LM}$, which raises an inner-shell electron to empty valence orbitals, is defined by

TABLE III. Electrostatic, exchange and spin-orbit parameters (in eV). The F and G integrals are scaled down to 80% of their Hartree-Fock values.

Ground state: $3d^{10}5f^n$											
		n		$F^2_{(f)}$		$F^4_{(f)}$		$F^6_{(f)}$		ζ_f	
U^{4+}		2		7.611		4.979		3.655		0.261	
Np^{3+}		3		7.434		4.834		3.538		0.270	
Excited state: $3d^9 5f^{n+1}$											
	n	$F^2_{(5f)}$	$F^4_{(5f)}$	$F^6_{(5f)}$	$F^2_{(5f,3d)}$	$F^4_{(5f,3d)}$	$G^1_{(5f,3d)}$	$G^3_{(5f,3d)}$	$G^5_{(5f,3d)}$	ζ_{3d}	ζ_{5f}
U^{4+}	2	8.020	5.258	3.865	2.051	0.952	1.603	0.969	0.678	73.384	0.301
Np^{3+}	3	7.861	5.125	3.757	2.033	0.943	1.588	0.960	0.672	77.311	0.312

$$J^{(e)}_{LM} = -\frac{4\pi i^L k^L}{(2L+1)!!}\sqrt{(L+1)/L}\sum_j er^L_j Y^L_M(\hat{\mathbf{r}}_j), \qquad (8)$$

with j running over all electrons. (We have assumed $T=0$.) Electric dipole transitions are identified by setting $L=1$ in the previous expressions.

In writing out the resonant amplitude, we have considered the simple case of a magnetic system with negligible crystal fields, that is cylindrical [SO(2)] symmetry. Equation (6) provides a suitable starting point for determining the form of the amplitude diffracted into any crystal point group.[30]

Going over to a 2×2 matrix representation of the amplitude f^{E1}, in the basis of two linearly independent polarization states (parallel and perpendicular to the scattering plane), the cross section for coherent elastic scattering is obtained from the definition[31]

$$\frac{d\sigma}{d\Omega} = \mathrm{Tr}\{F^\dagger_{E1}\rho F_{E1}\}, \qquad (9)$$

with ρ a density matrix, which describes the initial photon polarization in terms of the Stokes parameters, and

$$F_{E1}(\omega) = \sum_l e^{i\mathbf{K}\cdot\mathbf{R}_l} f^{E1}(\omega), \qquad (10)$$

where l runs over all ions, and $\mathbf{K}=\mathbf{k}-\mathbf{k}'$ denotes the scattering vector.

First-harmonic antiferromagnetic satellites are controlled by the polarization dependence $T^{(1)*}_0(\boldsymbol{\epsilon},\boldsymbol{\epsilon}'^*)_{E1} = -(i/\sqrt{2})(\boldsymbol{\epsilon}'^*\times\boldsymbol{\epsilon})$ and by the electronic operator $F^{(1)}_0(\omega)_{E1}$, in the resonant amplitude f^{E1}. For our two-ion model, the real and imaginary parts of f^{E1} were calculated as follows. The full U^{4+} and Np^{3+} multiplet structures were firstly determined in intermediate coupling using Cowan's programs.[32] (The Slater and spin-orbit parameters, which are relevant to our multiplet calculation, are listed in Table III. The absolute values for the energy have been scaled to those found experimentally, a shift of ~ 20 eV, to correct for the Hartree-Fock overestimation of the center of gravity of the multiplet.) Both ions where then embedded in a crystalline field by implementing the formalism of Butler,[33] as coded by Thole. In this framework, the crystal field perturbation is expressed as a linear combination of unit tensor operators U^{ka0} and reads

$$H_{\mathrm{c.f.}} = \sum_{ka} X^{ka0}U^{ka0}, \qquad (11)$$

with X^{ka0} a set of free parameters. For f electrons in D_{4h} symmetry, $k=2,4,6$ and $a=0,2$.

In the D_{4h} point group, the $5f^4$ configuration $J=4$ ground state of the Np^{3+} ion splits into $\Gamma_{t2},\Gamma_{t3},\Gamma_{t4},\Gamma^1_{t1},\Gamma^2_{t1},\Gamma^1_{t5},\Gamma^2_{t5}$ states, i.e., five singlets and two doublets. Similarly, for the $5f^2$ configuration $J=4$ ground state of U^{4+}. (The Hund's rule states of Np^{3+} and U^{4+}, $^3I_4$ and $^3H_4$, have purities 82 and 88 %, respectively.) In the absence of an experimental determination of the $5f$-level structure in the mixed alloys, our choice of the crystal-field parameters was guided by the knowledge of the neptunium magnetic moment and by the spectral shape of the resonant magnetic scattering. Most probably, this knowledge does not render the choice unique. The following values (in eV) for the crystal-field parameters were chosen: $X^{220}=0.05$, $X^{400}=0.093$, $X^{420}=-0.07$, $X^{600}=0.452$, and $X^{620}=0.99$, for U^{4+}; $X^{220}=0.01$, $X^{400}=0.6$, $X^{420}=-0.05$, $X^{600}=-0.01$, and $X^{620}=-0.1$, for Np^{3+}. The corresponding level distributions are given in Table IV.

In the calculation, the presence of an exchange interaction was simulated by turning on an external magnetic field coupled to ground-state spin only. This was achieved by adding the term $g\mu_B HS$ to the Hamiltonian, with $\mu_B H=0.01$ eV, thus reducing the point-group symmetry to C_{4h}. A core-hole width $\Gamma_{M_{IV}}=\Gamma_{M_V}=3.4$ eV [full width at half maximum (FWHM)] was assumed. To reproduce the experimental widths, a further convolution with a Gaussian line shape of standard deviation $\sigma=1.4$ eV was found necessary.

The above model is based on the premise that the neptunium moment is $\sim 1.5\mu_B$ and this is accurately reproduced in our calculations. The magnetic moment of the uranium

TABLE IV. Tetragonal crystal-field states for U^{4+} and $Np^{3+}(J=4)$.

Ion	U^{4+}		Np^{3+}	
State	E [meV]		State	E [meV]
$\lvert\Gamma_{t4}\rangle$	0		$\lvert\Gamma^1_{t5}\rangle$	0
$\lvert\Gamma^1_{t1}\rangle$	2		$\lvert\Gamma_{t4}\rangle$	11
$\lvert\Gamma_{t2}\rangle$	22		$\lvert\Gamma^1_{t1}\rangle$	38
$\lvert\Gamma_{t3}\rangle$	28		$\lvert\Gamma_{t3}\rangle$	56
$\lvert\Gamma^1_{t5}\rangle$	34		$\lvert\Gamma_{t2}\rangle$	63
$\lvert\Gamma^2_{t5}\rangle$	62		$\lvert\Gamma^2_{t5}\rangle$	64
$\lvert\Gamma^2_{t1}\rangle$	98		$\lvert\Gamma^2_{t1}\rangle$	88

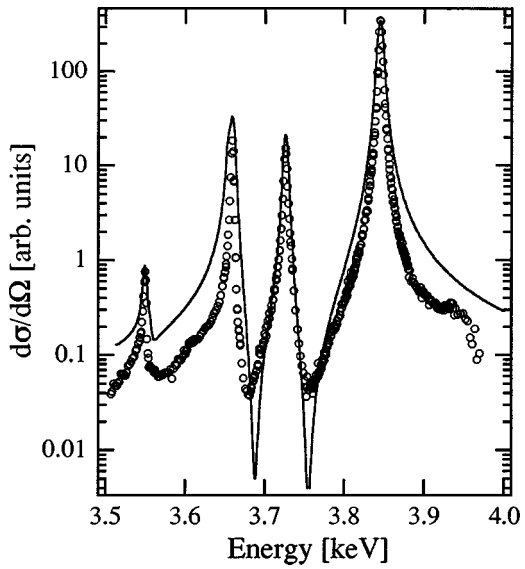

FIG. 7. Calculated resonant magnetic scattering cross section as a function of incident photon energy (solid line). The observed values of Fig. 6(b) have been multiplied by μ to compare with the calculations, The observed and calculated intensities have been normalized at the peak of the neptunium M_4 resonance. The calculated values descend further since they contain no background.

atom for the $x=0.5$ alloy is $0.42\mu_B$, which represents a strong increase over that found ($0.02\mu_B$) in URu_2Si_2.

A coherent superposition of the calculated scattering amplitudes leads to a resonant cross section as a function of photon energy as displayed in Fig. 7. To compare with the experimental observation we also display the experimental data multiplied by μ. We have argued in Sec. IV B that the proper correction at the peak of the resonant intensity should be μ^2 rather than μ, but this will reduce to μ as we move away from the resonant condition. Recalling that these plots are on a logarithmic scale, we prefer not to attempt to reproduce this effect, and use a correction based on μ for all photon energies. The agreement between the calculated values and the experimental ones is remarkably good.

B. Modelling the magnetization curve

To our knowledge this is the one of the first observations that there are different temperature dependencies of the magnetization for two atomic species occupying the same lattice sites in a random alloy. The effect of replacing uranium by neptunium in the lattice is twofold. First, the chemical translational symmetry is destroyed, although it is anticipated that because of the similarity between the elements, any chemical effects are minor and can be neglected. Secondly, as shown using Mössbauer spectroscopy[14] (see Fig. 2), the neptunium orders with a substantial magnetic moment that will affect the uranium. As the neptunium moments order, they create a molecular field that induces a sizable moment on the uranium site. The magnetic moment of the neptunium is known from Mössbauer spectroscopy to be $1.5\mu_B$. Thus, if we neglect other aspects, the effect of replacing some of the uranium in URu_2Si_2 with neptunium can be viewed as applying an *internal staggered* magnetic field and we can compare our data with those obtained in high magnetic fields on pure URu_2Si_2.

Sugiyama *et al.*[9] have studied the result of applying high magnetic fields on the pure uranium compound and a number of metamagnetic transitions were observed, starting at 35.8 T at 1.3 K, as the field was applied along the c-axis. In the model of Santini and Amoretti,[3,8] the order parameter in the pure URu_2Si_2 compound is of quadrupolar nature and the exchange integral does not result in a transferred exchange field. In pure $NpRu_2Si_2$, on the other hand, the ordering is dipole, as is usually the case, so that the exchange integral results in a polarization of neighboring dipoles. In a simple model of an antiferromagnet, the transition temperature can be written as $T_N=C(\Sigma_i W_i)$ where W_i is the exchange integral for the ith neighbor. C is the Curie constant. The molecular field on an atom becomes $B=(3T_Nk_B)/\mu_{Np}=82$ T at 0 K. A simple approach is therefore to suppose that the substitution of neptunium for uranium will act as a local molecular field on the uranium. This field will depend on the number of nearest neptunium neighbors.

We have calculated the temperature dependence of the uranium moments in the mixed compounds assuming that the field is transferred by the RKKY interaction. This has the form

$$F(z)=\frac{z\cos z-\sin z}{z^4}, \tag{12}$$

where $z=2k_Fr$. k_F is the Fermi vector and r is the distance. Sugiyama *et al.*[9] found that a value of $k_F=0.55$ Å^{-1} was compatible with their analysis of the magnetization data. We have used this value and calculated the influence on the uranium atoms in a lattice with a random distribution of neptunium atoms. We assume the interaction to be isotropic. This was found to be approximately the case by Palstra *et al.*[34] even though they obtained a value of 1 Å^{-1}. The field from the neptunium is deduced from the square root of the magnetization curves determined in our experiment. The uranium moments as a function of the applied field follow the curve obtained by Sugiyama *et al.*[9] Figure 8 shows the normalized calculated curve for $x=0.1$ together with the experimental data. The agreement is good. We obtain a moment of $0.34\mu_B$ at 10 K. The same calculation for the $x=0.5$ sample also gives reasonable agreement. In this case the calculated uranium moment reaches $1.1\mu_B$ at 12.5 K, thus much larger than that estimated above. The reason for this large moment is that for this composition the average field from the neptunium is 41 T i.e., larger than the value for which the moment shows a discontinuity in its value as a function of field. If, instead, we assume that the field in the pure neptunium compound is 50 T, we obtain a moment of $0.5\mu_B$ at 12.5 K for the $x=0.5$ alloy. The agreement with the measured uranium magnetization curve is not quite as good. In this case, the $x=0.1$ compound would have a uranium moment of only $0.1\mu_B$.

The present model thus provides one *possible* explanation of the temperature dependence of the uranium magnetization. A problem is that in the model, the saturated uranium

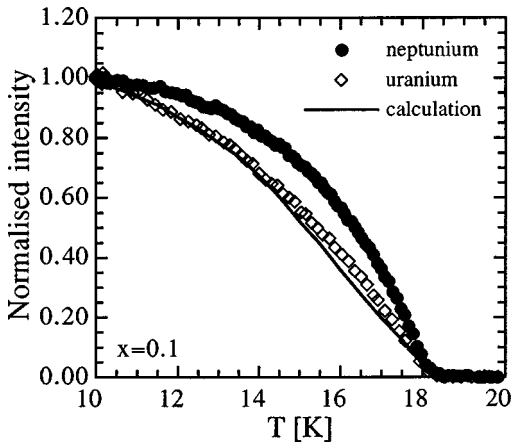

FIG. 8. A calculation the of uranium moment as a function of the temperature in the $x=0.1$ alloy following a model described in the text, which uses the measured variation of the neptunium moment as input.

moment is linearly dependent on x, while the experimental data point towards the moments being similar for $x=0.1$ and $x=0.5$.

VI. CONCLUSIONS

For $x=1$ ($NpRu_2Si_2$) we have confirmed previous neutron scattering results, but with much higher count rates and improved q resolution. Going beyond the results of the previous neutron scattering study,[12] we have followed the third-order harmonic as a function of temperature. We conclude that there is no $2q$ charge modulation induced by the magnetic ordering. From the width of the first-order satellite reflection we find a magnetic correlation length along the magnetic propagation direction **c** of only $\xi_c=650$ Å at 12.5 K, whereas it is truly long range for the commensurate compounds. The widths of the magnetic satellites in the $x=1$ sample grow as the temperature is lowered indicating competition between magnetic and elastic forces in the crystal. Our study gives a more exact and complete picture of the magnetism of this material than was previously available.

Using the element specificity of the method, we have found that the temperature dependencies of the uranium and the neptunium moments differ in the mixed $U_{1-x}Np_xRu_2Si_2$ solid solutions and we have presented some possible explanations for this behavior. The substitution of uranium by neptunium does not greatly perturb the lattice (see Fig. 2), but it does introduce a strong molecular field at the uranium sites as a result of the large moment of $1.5\mu_B$ carried by neptunium. There are at least two observable effects arising from the presence of this molecular field. First, it acts on the (initially at $x=0$) uranium moment of $0.02\mu_B$ to increase it by an order of magnitude. This implies a large susceptibility at the uranium site, which is proposed by Santini and Amoretti,[3] and already established by the high-field measurements of Sugiyama *et al.*[9] Second, for low values of this internal molecular field (i.e., $T\sim T_N$) the uranium site susceptibility is almost linear and the separate (and different) temperature dependencies may be modelled by a simple molecular field approach.

Theoretical calculations have been made of the resonant cross section in the $x=0.50$ sample. These calculations start by assuming the ground states of the uranium and neptunium ions. In particular, they assume U^{4+} and Np^{3+} ground states. The latter is consistent with the Mössbauer isomer shift, and the former is consistent with a number of models (Santini,[8] and references therein); however, it is inconsistent with the valence as derived from electronic structure calculations for such a uranium intermetallic.[11] Moreover, neutron inelastic experiments have failed to observe the crystal-field excitations suggested in Table IV (Ref. 6), so that we are aware that assuming a localized $5f^2$ model is a first approximation. Nevertheless, we are forced to start from this assumption as any state with a U^{3+} ground state is bound to have a considerable magnetic moment within the localized picture we are using. There is reasonable agreement between experiment and theory for the $x=0.5$ composition. The moment at the uranium site is $0.4\mu_B$. Assuming a simple linear relationship gives $0.3\mu_B$, so that we can assume the moment is of this order of magnitude, which is ~ 10 times greater than the $0.02\mu_B$ found in the $x=0$ pure compound.

Following the ideas of a localized state for the U^{4+} ground state, it is straightforward to postulate that the large moment on uranium sites for the $x>0$ compositions is because they sit in a molecular field from the surrounding (polarized below T_N) neptunium ions. Such a model explains the values of the uranium moments, and that they have a temperature dependence *different* from the neptunium sublattice. This difference can be simulated by a molecular field argument, but these models will obtain β values that are 1/2. To simulate the β parameters measured in the present experiment a more sophisticated approach is necessary.

One interesting aspect is that according to our measurements the moments induced on the uranium sites are approximately the *same* for both the $x=0.1$ and $x=0.5$ compositions. A molecular field argument, assuming a linear response at the uranium site, would suggest that the moment in the $x=0.5$ composition should be considerably greater than that in the $x=0.1$ composition. This is not yet understood.

We have demonstrated the feasibility of finding and studying the magnetic properties of small (<1 mg) actinide samples at a synchrotron radiation source and conclude that it is possible to further reduce the sample size, to investigate microgram samples and thin films. Count rates at the neptunium M_4 edge in excess of 50 000 cts/s are obtained at the ID20 beamline at the ESRF from a sample containing only 30μg of neptunium. The small size reduces the associated safety concerns considerably.

It would be interesting to extend this work to lower neptunium concentrations. From Wastin *et al.*[13] we know that the $x=0.01$ sample shows transport properties that are very close to those of the undoped ($x=0$) sample. Preparations for such experiments are under way.

ACKNOWLEDGMENTS

We thank P. Dervenagas for assistance in the early experiments. We acknowledge with gratitude the help with the safety aspects provided by P. Berkvens and P. Colomp of the ESRF Radioprotection group. Loading of the samples was

performed at the neighboring Institut Laue Langevin, and we thank the staff of Radioprotection at that Institute. We also acknowledge the help by L. Chabert in constructing monitoring equipment for the safety of the experiments. The high purity neptunium metal required for the fabrication of these compounds was made available through a loan agreement between Lawrence Livermore National Laboratory and ITU, in the frame of a collaboration involving LLNL, Los Alamos National Laboratory, and the US Department of Energy.

[1] T.T.M. Palstra, A.A. Menovsky, J. van den Berg, A.J. Dirkmaat, P.H. Kes, G.J. Niewenhuys, and J.A. Mydosh, Phys. Rev. Lett. **55**, 2727 (1985).

[2] B. Fåk, C. Vettier, J. Flouquet, F. Bourdarot, S. Raymond, A. Vernière, P. Lejay, Ph. Boutouille, N.R. Bernhoeft, S.T. Bramwell, R.A. Fischer, and N.E. Phillips, J. Magn. Magn. Mater. **154**, 339 (1996).

[3] P. Santini and G. Amoretti, Phys. Rev. Lett. **73**, 1027 (1994).

[4] M.B. Walker and W.J.L. Buyers, Phys. Rev. Lett. **74**, 4097 (1995).

[5] P. Santini and G. Amoretti, Phys. Rev. Lett. **74**, 4098 (1995).

[6] C. Broholm, H. Lin, P.T. Matthews, T.E. Mason, W.J.L. Buyers, M.F. Collins, A.A. Menovsky, J.A. Mydosh, and J.K. Kjems, Phys. Rev. B **43**, 12 809 (1991).

[7] B.R. Cooper, Phys. Rev. **163**, 444 (1967).

[8] P. Santini, Phys. Rev. B **57**, 5191 (1998).

[9] K. Sugiyama, H. Fuke, K. Kindo, K. Shimohata, A.A. Menovsky, J.A. Mydosh, and M. Date, J. Phys. Soc. Jpn. **59**, 3331 (1990).

[10] L.M. Sandratskii and J. Kübler, Phys. Rev. B **50**, 9258 (1994).

[11] M.S.S. Brooks, B. Johansson, and H.L. Skriver, in *Handbook of the Chemistry and Physics of the Actinides*, edited by A.J. Freeman and G. H. Lander (North-Holland, Amsterdam, 1984), Vol. 1, Chap. 3, p. 153.

[12] M. Bogé, D. Bonnisseau, P. Burlet, J.M. Fournier, E. Pleska, S. Quezel, J. Rebizant, J. Rossat-Mignod, J.C. Spirlet, and M. Wulff, J. Nucl. Mater. **166**, 77 (1989).

[13] F. Wastin, E. Bednarczyk, J. Rebizant, S. Zwirner, and G.H. Lander, J. Alloys Compd. **262–263**, 124 (1997).

[14] S. Zwirner, J.C. Waerenborgh, F. Wastin, J. Rebizant, J.C. Spirlet, W. Potzel, and G.M. Kalvius, Physica B **230–232**, 80 (1997).

[15] W. Potzel, G.M. Kalvius, and J. Gal, in *Handbook of the Chemistry and Physics of Rare Earths*, edited by K.A. Gschneidner, L. Eyring, G.H. Lander, and G.R. Choppin (Elsevier, Amsterdam, 1993), Vol. 17, Chap. 116.

[16] P. Dervenagas, A. Hiess, G.H. Lander, F. Wastin, and J. Rebizant, Solid State Commun. **109**, 35 (1999).

[17] D.B. McWhan, C. Vettier, E.D. Isaacs, G.E. Ice, D.P. Siddons, J.B. Siddons, C. Peters, and O. Vogt, Phys. Rev. B **42**, 6007 (1990).

[18] J.P. Hannon, G.T. Trammel, M. Blume, and D. Gibbs, Phys. Rev. Lett. **61**, 1245 (1988).

[19] J. Rossat-Mignod, G.H. Lander, and P. Burlet, in *Handbook of the Chemistry and Physics of the Actinides*, edited by A.J. Freeman and G.H. Lander (North-Holland, Amsterdam, 1984), Vol. 1, Chap. 6, p. 415.

[20] J.O. Dimmock, Phys. Rev. **130**, 1337 (1963).

[21] G. Helgesen, J.P. Hill, T.R. Thurston, Doon Gibbs, J. Kwo, and M. Hong, Phys. Rev. B **50**, 2990 (1994).

[22] J.D. Axe, in *Physics of Structurally Disordered Solids, NATO Advanced Studies Institutes Series*, edited by S.S. Mitra (Plenum, New York, 1976), p. 507.

[23] N. Bernhoeft, Acta Crystallogr., Sect. A: Found. Crystallogr. **55**, 274 (1999).

[24] M. Blume, in *Magnetic Effects in Anomalous Dispersion*, edited by G. Materlik, C.J. Sparks, and K. Fischer (Elsevier Science, Amsterdam, 1994), p. 495.

[25] J. Luo, G.T. Trammell, and J.P. Hannon, Phys. Rev. Lett. **71**, 287 (1993).

[26] A. Vigliante, M.J. Christensen, J.P. Hill, G. Helgesen, S. Aa Sørensen, D.F. McMorrow, Doon Gibbs, R.C.C. Ward, and M.R. Wells, Phys. Rev. B **57**, 5941 (1998).

[27] J.O. Cross, M. Newville, J.J. Rehr, L.B. Sorensen, C.E. Bouldin, G. Watson, T. Goulder, G.H. Lander, and M.I. Bell, Phys. Rev. B **58**, 11 215 (1998).

[28] D. Mannix, S. Langridge, G.H. Lander, J. Rebizant, M.J. Longfield, W.G. Stirling, W.J. Nuttal, S. Coburn, S. Wasserman, and L. Soderholm, Physica B **262**, 125 (1999).

[29] C.C. Tang, W.G. Stirling, G.H. Lander, Doon Gibbs, W. Herzog, Paolo Carra, B.T. Thole, K. Mattenberger, and O. Vogt, Phys. Rev. B **46**, 5287 (1992).

[30] P. Carra and B.T. Thole, Rev. Mod. Phys. **66**, 1509 (1994).

[31] M. Blume and D. Gibbs, Phys. Rev. B **37**, 1779 (1988).

[32] R.D. Cowan, *The Theory of Atomic Structure and Spectra* (University of California Press, Berkeley, 1981).

[33] P.H. Butler, *Point Group Symmetry Applications — Methods and Tables* (Plenum Press, New York, 1981).

[34] T.T.M. Palstra, A.A. Menovsky, and J.A. Mydosh, Phys. Rev. B **33**, 6527 (1986).